Bull. Mater. Sci., Vol. 40, No. 6, October 2017, pp. 1081–1086
DOI 10.1007/s12034-017-1447-4

Stability, magnetic and electronic properties of SiC sheet doped with B, N, Al and P

L B DRISSI[1,2,*] and F EL YAHYAOUI[1]

[1]LPHE, Modeling and Simulations, Faculty of Science, Mohammed V University in Rabat, Rabat, Morocco
[2]CPM, Centre of Physics and Mathematics, Faculty of Science, Mohammed V University in Rabat, Rabat, Morocco
*Author for correspondence (ldrissi@fsr.ac.ma)

MS received 2 September 2016; accepted 25 January 2017; published online 6 September 2017

Abstract. Using DFT-based calculations, we study chemical doping of silicene–graphene hybrid with (B, N, Al and P). Planar structure of SiC sheet remains unaffected on doping and all the systems are stable. P and N dopants are strongly bonded to the hybrid compared with Al and N. Charge transfer calculations show that (B, N)/(Al, P) behave like acceptors/donors, respectively. All configurations retain the semi-conductor character of pure SiC and show magnetic order. Curie temperature is determined for the ferromagnetic structures. These results provide the possibility of tuning the gap and inducing magnetism in SiC as required for future applications.

Keywords. Silicene–graphene; *ab-initio* calculations; substitution; magnetic properties; electronic structure; Bader analysis.

1. Introduction

Recently, silicene, the Si analogue of graphene, was chemically exfoliated from calcium disilicide ($CaSi_2$) [1]. Silicene shows a small out-of-plane distortion and forms a slightly buckled structure [2–4]. This buckling enhances chemical reactivity of silicene and lowers its point group symmetry [5]. The origin of this non-planarity is attributed to pseudo-Jahn–Teller distortions [6], which are much more prominent in germanene compared with silicene as discussed in light of vibronic coupling between the electronic states [7].

Similar to graphene, silicene is a zero-gap semiconductor with π and π^* bands crossing linearly at K- and K′-points at the Fermi level, giving a massless Dirac fermion character to charge carriers [8,9]. Using a compiled set of LEED, CLs and ARPES data, it was found that silicene layer is in contact with the bands derived from Ag(111) silver surface at several Γ-points with a band velocity of 1.3×10^6 m s^{-1} and a gap of 0.3 eV [10,11]. Linear dispersion observed by ARPES experiments [11] and scanning tunnelling spectroscopy [12] for silicene–Ag(111) originates primarily from the Ag-substrate and not from Dirac cone in silicene as it is destroyed by distortions and interactions with Ag surface [13,14].

Both graphene and silicene are non-magnetic (NM) materials. To adapt them to applications in spintronic and magnetic storage, it is of fundamental importance to introduce magnetism. To address this issue in graphene, several works have focussed on reduced dimensionality [15]. In this approach, the magnetism is due to edge effects. This is particularly the case for structures with zigzag edges such as zigzag graphene nanoribbons, where antiferromagnetic (AFM) order is across edges [16], and zigzag-edged triangular graphene nanoflakes, where a large net spin is observed [17]. Chemical functionalization is another efficient way to tune magnetic properties in 2D carbon sheets. In particular, it has been reported that chemisorption of single hydrogen atom creates magnetic graphene [18] and one-sided surface modification with hydrogen induces long-range ferromagnetic (FM) order [19].

Although the free-standing silicene sheets have not been isolated yet, several theoretical works have been explored in advanced ways to transform Si sheets into a magnetic semiconductor. In a manner similar to that in graphene, magnetic ordering in silicene is explained by the presence of impurities, boundaries or defects. Among these fundamental issues, ferromagnetism is achieved upon partial hydrogenation/bromination that breaks π-bonding network in Si-sheets [20,21]. Silicon adatoms as self-dopants in silicene result in a long-range magnetic order due to unpaired electrons from the off-plane Si atoms [22]. Moreover, a substantial magnetic moment is found in di-vacancy silicene as well as in doped sheet with aluminium, phosphorous [23] and boron [24].

Si–C sheet, a two-dimensional planar sheet with sp^2 hybridization, at the expense of sp^3 hybridization, has attracted significant interest [25–27]. Due to sublattice asymmetry in its honeycomb lattices, SiC hybrid is a non-zero-gap semi-conductor [25,27]. The analysis of optical absorption spectra reveals that excitonic effects in silicene–graphene hybrid are significant and lead to strongly bound excitons [28]. Complete hydrogenation of silicene–graphene surface yields five stable and buckled structures having an insulating

character [29]. Partial H coverage reduces the initial gap of SiC hybrid in favour of ferromagnetism [27].

SiC nanosheets were synthesized by sonication of SiC powders in polar solutions, such as N-methylpyrrolidone (NMP) and isopropyl alcohol (IPA) for 24 h [30]. This semiconductor compound exhibits outstanding light-emitting ability in its photoluminescence spectra, which opens a new door to LEDs. For developing novel materials, it is very useful to tailor physical properties of SiC monolayer. In this paper, motivated by previous works on graphene and silicene, we study the effect of adding foreign atoms containing less or more electrons, such as B, N, Al and P, on pure SiC hybrid. We focus our interest on structural parameters, binding energies, electronic and magnetic properties of configurations where a single C atom is substituted with a B or an N atom, and also the structures where we replace one Si atom by P or Al atom. Using *ab-initio* calculations within the density-functional theory (DFT), it is found that the planar structure of the SiC sheet remains unaffected on doping and all the relaxed systems with substituted atoms are stable. The P and N dopants are strongly bonded to the hybrid compared with Al and N. The charge transfer calculations show that due to the elements electronegativity, B and N behave like acceptors while P and Al atoms behave as donors. All the configurations retain the semi-conductor character of pure SiC. Our calculations show that the B, Al and P substituents reduce the initial band gap in SiC with the smallest gap of 1.58 eV observed for B atom, and only N increases the gap energy. Except P–SiC, which shows an AFM order with an indirect band gap, the remaining structures B–SiC, N–SiC and Al–SiC are FM semi-conductors with direct band gap.

2. Computational details

All the calculations have been performed using the Quantum espresso (QE) simulation package [31] and DFT formalism employing generalized gradient approximation GGA-DFT of Perdew–Burke–Ernzrhoff (PBE) exchange-correlation functional [32]. An ultra-soft pseudo-potential description of electron–electron is used with $2s^2 2p^2$, $3s^2 3p^2$ and $1s^1$ valence electron configurations for C, Si and H atoms, respectively. We apply a plane-wave basis set for electronic wavefunctions and charge density, with kinetic energy cut-off of 40 and 400 Ry, respectively. In the reciprocal space, following the Monkhorst–Pack scheme [33], Brillouin-zone integration was carried out at $8 \times 8 \times 1$ k-points in geometry optimization calculations, and $14 \times 14 \times 1$ k-point grids were used to obtain the electronic properties. We relax all the structures using a criterion of forces and stresses on atoms, until the energy change is smaller than 10^{-4} eV. To calculate charge density and spin moment, we have employed Bader population analysis [34]. Using these computational details, we describe the corresponding crystallographic structures and give electronic character and magnetic properties of SiC sheet chemically doped with B, N, Al or P. Calculated parameters are listed in table 1.

Table 1. Calculated parameters for B-, N-, Al- and P-substituted SiC: bond length d between the substituent and its first nearest neighbours in Å; binding energy E_B and gap energy E_g in eV; Curie temperature T_C in K and charge located on substituent in e [$(-qe)$ denotes electron lost and (qe), gained].

Substituent	d	E_B	E_g	T_C	q
B	1.89	−1.36	1.58	189.16	1.11
N	1.75	−4.33	2.60	280.84	1.7
Al	1.90	−1.51	2.32	110.04	−0.08
P	1.73	−7.36	1.81	—	−0.05

3. Results and discussion

3.1 *Structural properties*

Silicene–graphene sheet is a one-atom-thick silicon and carbon arranged in a honeycomb lattice in which carbon atoms are in A sites and silicon atoms are in B sites of the hexagonal structure. According to [27], the SiC hybrid is a zero-buckle monolayer with bond length $(d_{C-Si} = 1.78\,\text{Å})$. To keep the structure of SiC planar and to avoid dopant-atom clustering on the SiC sheet, we consider configurations with at most one substituent for each hexagonal ring [35]. To do so, we substitute a single C atom by B or N atom or we replace one Si atom by P or Al atom as shown in figure 1. The nearly same size of C or Si and their host ensures that there is no significant distortion in the SiC structure. From the structural data, the buckle parameter is $\Delta = 0$ in the four configurations and the C–Si bond length remains constant ($d_{C-Si} = 1.78\,\text{Å}$). Both of the interatomic distances ($d_{B-Si} = 1.89\,\text{Å}$) and ($d_{C-Al} = 1.90\,\text{Å}$) are larger than the bond lengths d_{C-Si}; however, the lengths ($d_{C-P} = 1.73\,\text{Å}$) and ($d_{N-Si} = 1.75\,\text{Å}$) are slightly shorter compared with d_{C-Si}. This results in good agreement with [36] and [24], where the interatomic distances are longer for column III dopants compared with column V dopants.

3.2 *Stability analysis*

Binding energies corresponding to substitutional doping are obtained, by SCF energy calculations of the optimized structures, using the following expression [24]:

$$E_B = E_T - \left(\frac{N}{N-1}\right) E_{SiC} - E_{dopant},$$

where N is the total number of C and Si atoms in pure SiC, E_T is the total energy of the substituted system and E_{SiC} is the atomic energy of pristine SiC sheet. It is found that SiC doped with B shows the lowest absolute value for binding energy in comparison with the other substituted atoms. The calculated values reveal that the substitution of a single B or N atom in SiC sheet occurs with a −1.36 and −4.33 eV

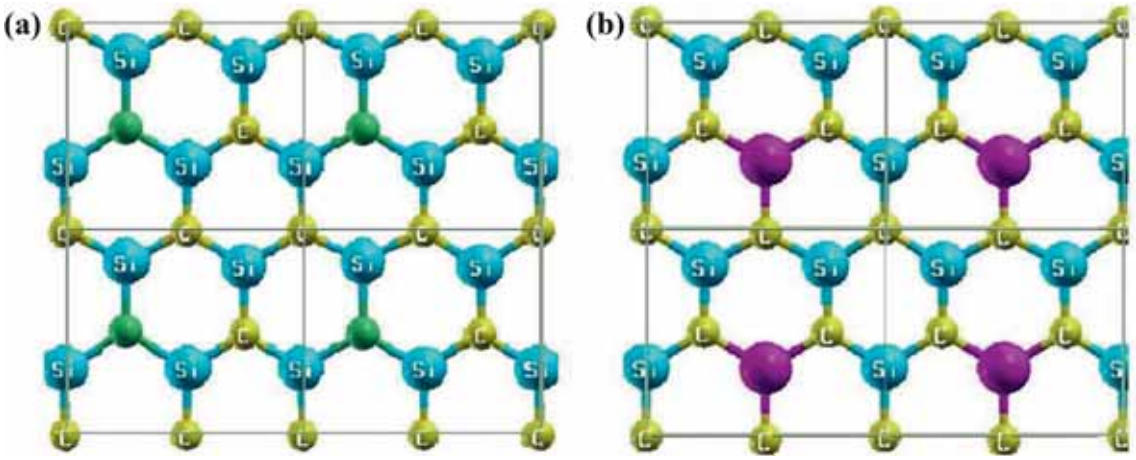

Figure 1. Supercell structure of doped silicene–graphene hybrid: (**a**) the green ball refers to B or N, substituted C atom and (**b**) the purple ball refers to Al- or P-substituted Si atom.

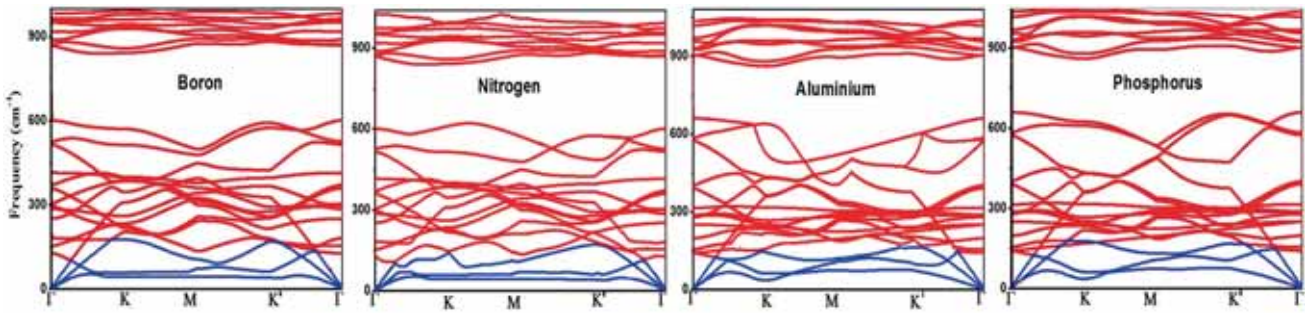

Figure 2. Phonon dispersion corresponding to configurations with B and P dopants. Blue and red branches refer to the 3 acoustic and 21 optical modes, respectively.

binding energy, respectively, in good agreement with −1.77 (−4.56) eV obtained in B (N)-adsorbed graphene [37]. The binding strengths $E_B = -1.51$ and −7.36 eV, for Al- and P-atom-doped SiC monolayer, respectively, are of the same magnitude as the binding energies −2.28 and −4.84 eV of silicene doped with Al and P [24]. All the binding energies have negative values, which indicates that the four structures are stable. The absolute values of binding energy are considerably large for column V dopants (N and P) compared with column III dopants (B and Al). This result was expected because the long interatomic distances between column III dopants and their host neighbours indicate that they form weaker bonds compared with column V dopants. It follows that binding energy tends to reduce when the bond distances are larger [36,37]. Moreover, for dopants from the same column, $|E_B|$ showed a tendency to increase in structures with Si doping compared with C-doped structures. This is in good agreement with results on SiC sheet doped with 3d-transition metals [38].

The phonon dispersion plotted in figure 2 for SiC with B and P dopants shows the absence of imaginary frequency along any high-symmetry direction of the Brillouin zone. This result confirms the stability of the considered structures. The two curves display 3 acoustic branches and 21 optical ones, where optical modes fall in the frequency range of acoustic branches. According to [25], this is a property of 2D honeycomb structures containing at least one element from the first row of the periodic table. The highest vibrational frequencies are observed at 997.30 and 1084.49 cm^{-1} in B and P configurations, respectively, and at 1011.30 and 1025.04 cm^{-1} in Al and N configurations, respectively, which is consistent with pristine SiC having the maximum vibrational frequency around 1000 cm^{-1} [28].

3.3 *Charge transfer*

For boron-doped SiC sheet, the electrons are transferred from the silicon atoms to B and C atoms. The Bader analysis revealed that Si loses an amount of its electronic charge while its nearest neighbours C and B atoms gain 0.2 and 1.11e, respectively. Upon N substitution, Si donates electronic charges to C and N atoms that gain 0.1 and 1.7e, respectively. A similar behaviour is found for silicene lattice [24]; the calculated charge transfers from silicene to the substitutional doping B, N, Al and P are 1.4, 2.1, −1.6 and 1.2e, respectively. This charge transfer character is due to the

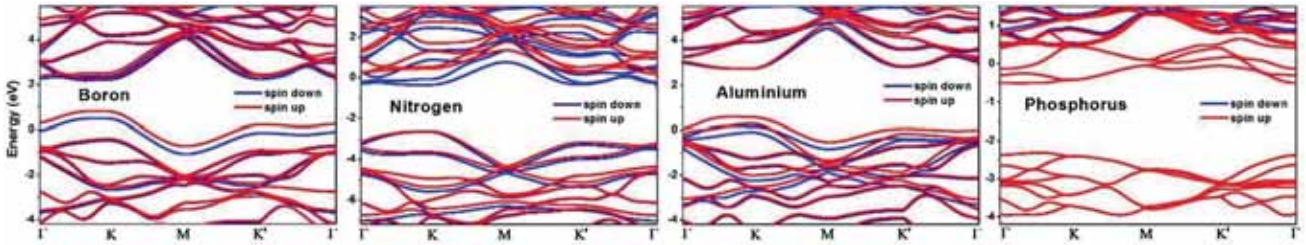

Figure 3. The calculated band structures of B-, N-, Al- and P-substituted silicene–graphene sheet.

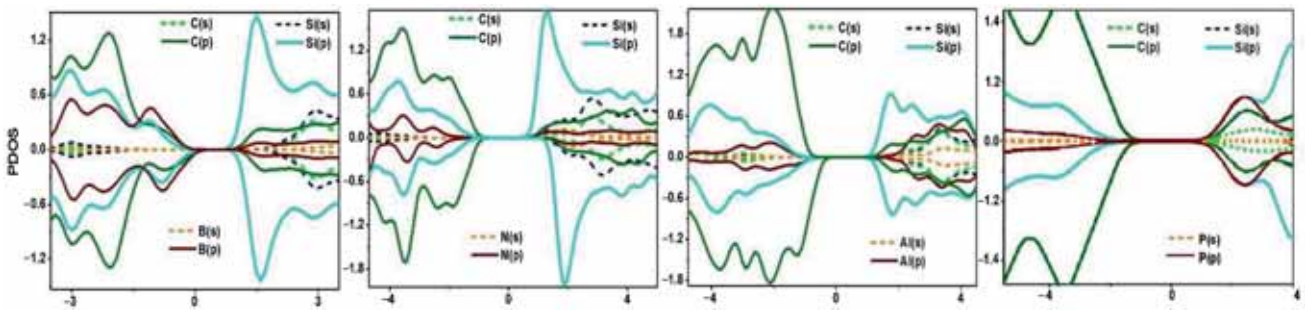

Figure 4. The partial density of states (PDOS) of B-, N- and Al-substituted silicene–graphene sheet. The Fermi energy is used as the origin of the energy scale.

differences of electronegativity among the atoms. Indeed, the Pauling electronegativity of Si atom ($\eta_{Si} = 1.90$ eV) is lower than that of B ($\eta_N = 2.04$ eV), carbon ($\eta_C = 2.55$ eV) and N ($\eta_N = 3.04$ eV), which has the highest value. However, due to the high electronegativity of C atom compared with Si, Al ($\eta_{Al} = 1.60$ eV) and P ($\eta_P = 2.2$ eV) atoms, the Bader charge indicates that the charge transfer occurs from Al/P and Si atoms to their carbon neighbours for the two systems Al/P-doped SiC. The net charges located on Al and Si in Al-doped SiC are 0.08 and 0.06e, respectively. The net charge located on P and Si in SiC substituted by P has a value of 0.05 and 0.07e, respectively.

3.4 *Electronic structures*

Recall that pure silicene–graphene hybrid is a semiconductor with a direct band gap of 3.48 eV in K point calculated using many-body perturbation theory within GW [28]. Smaller gaps of 2.48 [28] and 2.52 eV [25] are found using LDA and GGA DFT approximations, respectively, which are known to underestimate the band gap. On doping, all the configurations show a semi-conducting nature as plotted in figure 3 using GGA with a direct gap at the K point of Brillouin zone for SiC substituted by single B, N and Al and indirect gap in P–SiC conformer. The largest gaps are observed for N with $E_N = 2.60$ eV, followed by Al with $E_{Al} = 2.32$ eV. When doped with P and B, the band gaps are 1.81 and 1.58 eV, respectively. Notice that except for nitrogen, the band gaps for B, Al and P are smaller than that of the corresponding pristine configuration.

For a reliable description of electronic structure, figure 4 shows the projected density of states (PDOS). The analysis of states around Fermi level shows that in B-doped SiC, conduction band belongs mainly to Si-p orbitals while the upper energy levels of valence band have contribution by both B-p and C-p orbitals. In N–SiC and Al–SiC, it is clear that the states around Fermi level belong mainly to C-p orbitals in valence band and to Si-p orbitals in conduction band. The PDOS shows the same behaviour for P–SiC in valence band, while the lower energy of the conduction band is primarily due to p-orbitals of P-atoms. Notice that the magnetism is relevant in B-, N-, and Al-doped SiC.

3.5 *Magnetic properties*

The analysis of the electronic band structure near the Fermi level (figure 3) confirms that doping SiC sheet with N, B, P and Al atoms induces magnetism. The asymmetrical spin-up and spin-down bands (in the valence band for the B and Al substituents and in the conduction band for the N and P dopants) indicate that the spin degeneracy is broken. To determine the preferred magnetic configurations for these doped hybrids, we run spin-polarized calculations in a 4×4 supercell for the three magnetic coupling configurations, namely, the NM coupling, the AFM ordering and the FM coupling. For B-, N- and Al-doped SiC sheets, the energy ordering is FM < AFM < NM. Therefore, SiC doped by B, N or Al exhibits an FM behaviour with energy differences of ($E_{AFM} - E_{FM} = 16.36$ meV) and ($E_{NM} - E_{FM} = 34.42$ meV) for B, ($E_{AFM} - E_{FM} = 9.5$ meV) and ($E_{NM} - E_{FM} = 15.4$ meV) for Al and

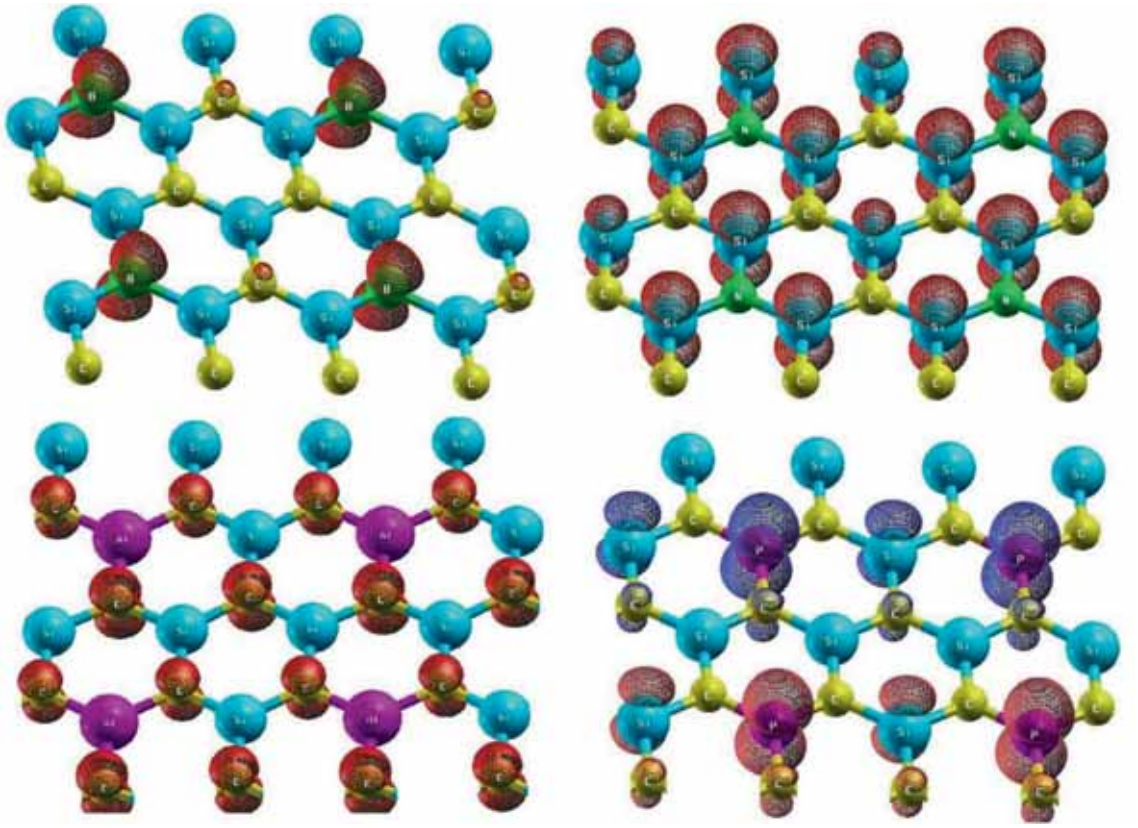

Figure 5. Spin density of B-, N-, Al- and P-substituted silicene–graphene sheet.

($E_{\mathrm{AFM}} - E_{\mathrm{FM=24.2\,meV}}$) and ($E_{\mathrm{NM}} - E_{\mathrm{FM}} = 285$ meV) for N. In [24], N-doped silicene induces also FM order. Moreover, the energy difference, between FM and AFM, is found to be 68 meV in half-hydrogenated silicene, which shows long-range FM order [39].

For our FM systems, Curie temperature, which is a critical parameter at which FM–paramagnetic transition occurs, is given by the formula [40]

$$\gamma K_{\mathrm{B}} T_{\mathrm{C}} = E_{\mathrm{AFM}} - E_{\mathrm{FM}},$$

where the dimension of the system is 2 and K_{B} is the Boltzmann constant. The corresponding Curie temperature is 189.16, 280.84 and 110.04 K for SiC doped by B, N and Al, respectively. This result is comparable to 100 K reported for FM graphene oxide doped with nitrogen [41] and to 121.6 and 144.8 K obtained, respectively, in one-side semi-hydrogenated silicene and germanene [42]. In half-brominated GeSi hybrid, T_{C} is estimated to be 340 K by adopting mean-field approximation, which reduced to 240 K on performing Monte Carlo simulations [43]. Moreover, our calculated T_{C} are consistent with respect to other 2D binary compounds, namely FM semi-hydrogenated group-IV monolayers SiGe-H, H-GeC and H-SiC exhibiting Curie temperatures of 108.9, 298.2 and 344.7 K, respectively [44].

In the remaining P-doped SiC structure, the AFM state has the lowest energy as the differences between energies per unit cell are ($E_{\mathrm{FM}} - E_{\mathrm{AFM}} = 6.7$ meV) and ($E_{\mathrm{NM}} - E_{\mathrm{AFM}} = 77.6$ meV). The same magnetic behaviour is found in half-brominated silicene as the AFM state lies 170 and 510 meV from the FM and NM states, respectively [39].

The distribution of spins is plotted in figure 5, where blue and red colours show the up- and down-spin directions. In N- and Al-doped SiC, the substituents are minor contributors, carrying negligible magnetic moment of 0.005 μ_{B} per atom for N and 0.002 μ_{B} per atom for Al. The induced magnetic moments are mainly localized on Si in N–SiC structure with a magnitude of 0.27 μ_{B} per atom and on carbon atoms in Al–SiC configuration with 0.21 μ_{B} per atom. This result is in good agreement with PDOS presented in figure 4, where the asymmetry between spin-up and spin-down states is significantly observed for Si(p)-orbitals in N–SiC and for C(p)-orbitals in Al–SiC. These values are of the same magnitude as the local moment 0.29 and 0.38 μ_{B} observed in the presence of B-vacancy and N-adatom defect in hexagonal boron nitride, respectively [45].

The situation is completely different for B–SiC and P–SiC configurations. Indeed, the density of spin is mainly located around the substituent atoms. Bader's spin analysis shows a contribution of 0.176 μ_{B} per atom for B atoms, which is very large compared with the small magnetic moment

found for carbon and silicon. In P–SiC configuration, carbon atoms contribute negligible spin moment of $0.002\,\mu_B$ per atom followed by $0.023\,\mu_B$ per silicon and significant magnitude of $0.144\,\mu_B$ per atom for P dopants. These values are in agreement in P-doped graphene, where spin density around the P atom is much larger than that around C atoms [46]. In this material, the global spin polarization is $1.05\,\mu_B$, while in silicene the adsorbed P atom on hill site has a net magnetic moment of $0.5\ \mu_B$ and the sum of induced magnetic moment on N-doped silicene is $0.9\,\mu_B$ [24]. Notice also that the conformer P–SiC shows an equal density of spin up and spin down, which certifies its AFM order.

4. Conclusion

In the present work, we have studied, using *ab-initio* calculations, internal structural parameters, band gap energy and magnetic properties of SiC sheet doped with single atoms (B, N, Al or P). All the structures are dynamically stable in the ground state and the largest binding energy is found for P followed by Al. Upon N or B substitution, the charge transfer occurs from the silicon atoms towards its neighbours. On doping with Al or P, only C atoms behave as acceptors of the electronic charge. This character is ascribed to the electronegativity of the atoms. The chemical doping of SiC monolayer with nitrogen increases the initial gap of pure SiC to 2.60 eV and has the largest Curie temperature of 280 K. In Al- and B-doped SiC, the initial gap is reduced to 2.32 and 1.58 eV, respectively, in favour of ferromagnetism. The energy gap is estimated to be 1.81 eV for P substituent, which is the major contributor carrying significant magnetic moment, leading to an AFM configuration. Our work reveals that the chemical doping with B, N, Al and P atoms is an efficient way to tune both the electronic and magnetic properties of SiC sheet for future nanoelectronics and spintronics.

Acknowledgement

We acknowledge the financial support from Centre National pour la Recherche Scientifique et Technique (CNRST)—Morocco.

References

[1] Nakano H *et al* 2006 *Angew. Chem.* **118** 6451
[2] Takeda K and Shiraishi K 1994 *Phys. Rev. B* **50** 14916
[3] Zhang M *et al* 2003 *Chem. Phys. Lett.* **379** 81
[4] Durgun E, Tongay S and Ciraci S 2005 *Phys. Rev. B* **72** 075420
[5] Jose D and Datta A 2012 *J. Phys. Chem. C* **116** 24639
[6] Soto J R, Molina B and Castro J J 2015 *Phys. Chem. Chem. Phys.* **17** 7624
[7] Nijamudheen A, Bhattacharjee R, Choudhury S and Datta A 2015 *J. Phys. Chem. C* **119** 3802
[8] Guzmán-Verri G G, Lew L C and Voon Y 2007 *Phys. Rev. B* **76** 075131
[9] Cahangirov S *et al* 2009 *Phys. Rev. Lett.* **102** 236804
[10] Avila J, De Padova P, Cho S, Colambo I, Lorcy S, Quaresima C *et al* 2013 *J. Phys. Condens. Matter* **25** 262001
[11] Vogt P, De Padova P, Quaresima C, Avila J, Frantzeskakis E, Asensio M C *et al* 2012 *Phys. Rev. Lett.* **108** 155501
[12] Chen L, Liu C C, Feng B, He X, Cheng P, Ding Z *et al* 2012 *Phys. Rev. Lett.* **109** 056804
[13] Wang Y-P and Cheng H-P 2013 *Phys. Rev. B* **87** 245430
[14] Gori P, Pulci O, Ronci F, Colonna S and Bechstedt F 2013 *J. Appl. Phys.* **114** 113710
[15] Bhowmick S and Shenoy V B 2008 *J. Chem. Phys.* **128** 244717
[16] Son Y-W, Cohen M L and Louie S G 2006 *Nature (London)* **444** 347
[17] Fernandez-Rossier J and Palacios J J 2007 *Phys. Rev. Lett.* **99** 177204
[18] Zhou J, Wu M, Zhou X and Sun Q 2009 *Appl. Phys. Lett.* **95** 103108
[19] Zhou J *et al* 2009 *Nano Lett.* **9** 3867
[20] Zheng F and Zhang C 2012 *Nanoscale Res. Lett.* **7** 422
[21] Zhang C W and Yan S S 2012 *J. Phys. Chem. C* **116** 4163
[22] Gao C, Zhang J, Liu H, Zhang Q and Zhao J 2013 *Nanoscale* **5** 9785
[23] Majumdar A, Chowdhury S, Nath P and Jana D 2014 *RSC Adv.* **4** 32221
[24] Sivek J, Sahin H, Partoens B and Peeters F M 2013 *Phys. Rev. B* **87** 085444
[25] Sahin H *et al* 2009 *Phys. Rev. B* **80** 155453
[26] Bekaroglu E *et al* 2010 *Phys. Rev. B* **81** 075433
[27] Drissi L B *et al* 2012 *J. Phys. Condens. Matter* **24** 485502
[28] Drissi L B and Ramadan F Z 2015 *Phys. E* **68** 38
[29] Drissi L B *et al* 2015 *Comput. Mater. Sci.* **96** 165
[30] Lin S 2012 *J. Phys. Chem. C* **116** 3951
[31] Giannozzi P *et al* 2009 *J. Phys. Condens. Matter* **21** 395502
[32] Perdew J P, Burke J P and Ernzerhof M 1996 *Phys. Rev. Lett.* **77** 3865
[33] Monkhorst H J 1976 *Phys. Rev. B* **13** 188
[34] Bader R F W 1991 *Chem. Rev.* **91** 893
[35] Krasnov P O, Ding F, Singh A K and Yakobson B I 2007 *J. Phys. Chem. C* **111** 17977
[36] Denis P A 2010 *Chem. Phys. Lett.* **492** 251
[37] Nakada K and Ishii A 2011 *Solid State Commun.* **151** 13
[38] Javan M B 2016 *J. Magn. Magn. Mater.* **401** 656
[39] Zheng F and Zhang C 2012 *Nanoscale Res. Lett.* **7** 422
[40] Kurz P, Bihlmayer G and Blugel S 2002 *J. Phys. Condens. Matter* **14** 6353
[41] Liu Y *et al* 2013 *Sci. Rep-UK* **3**
[42] Wang X, Li H and Wang J 2012 *Phys. Chem. Chem. Phys.* **14** 3031
[43] Zhang R-W, Zhang C-W, Li S-S, Ji W-X, Wang P-J, Li F *et al* 2014 *Solid State Commun.* **191** 49
[44] Yu W-Z, Yan J-A and Gao S-P 2015 *Nanoscale Res. Lett.* **10** 351
[45] Yang J, Kim D, Hong J and Qian X 2010 *Surf. Sci.* **604** 1603
[46] Dai J and Yuan J 2010 *J. Phys. Condens. Matter* **22** 225501